Applied Mathematical Modelling 34 (2010) 2644–2653

Contents lists available at ScienceDirect

Applied Mathematical Modelling

journal homepage: www.elsevier.com/locate/apm

# Modelling of recrystallization behavior and austenite grain size evolution during the hot rolling of GCr15 rod

Chong-xiang Yue [a], Li-wen Zhang [a,*], Jin-hua Ruan [a], Hui-ju Gao [b]

[a] School of Materials Science and Engineering, Dalian University of Technology, Dalian 116085, China
[b] Dongbei Special Steel Group, Dalian 116031, China

ARTICLE INFO

*Article history:*
Received 9 April 2009
Received in revised form 24 November 2009
Accepted 2 December 2009
Available online 6 December 2009

*Keywords:*
GCr15 steel
Microstructure evolution
Hot rod rolling
Recrystallization
Austenite grain size

ABSTRACT

In this paper, four 3-D finite element models are developed to simulate the whole rod rolling process of GCr15 steel. The distribution and evolution of different field-variables, such as effective strain, effective strain rate and temperature, are obtained. Based on the simulated results and the microstructure evolution models of the steel, the paper designs a FORTRAN program to predict the evolution of recrystallization behavior and austenite grain size in rolled piece during the rolling. The surface temperatures of rolled piece calculated by FEM agree well with measured values. Comparison between calculated values and measured ones of grain size shows the validity of the program.



## 1. Introduction

The microstructure after the rolling and cooling operations can control the properties of products [1]. So the study on the microstructure evolution during industrial hot rolling is important for steel industry to predict the mechanical properties of hot-rolled products, design the most effective processing path to fulfill quality requirements, and reduce the costs for the development of new products [2]. There are still many difficulties to precisely simulate the hot rolling process by laboratory experimental approach, and therefore, simulating the microstructure evolution using the numerical method becomes very meaningful [3].

Early in the 1970s, Sellars and his co-workers [4] at the University of Sheffield pioneered the concept that the complex microstructure processes occurring during hot rolling and subsequent cooling could be mathematically modelled. They [1,4,5] developed a set of models for thermo-mechanical processing of strip and applied the models to simulate the rolling of C–Mn steel. After the innovatory work, Kuziak [6] used the generalized plane strain approach to predict the distribution of deformation parameters and the evolution of austenite microstructure in the eutectoid steel workpiece during hot rod rolling. Sun [2] used a FDA (finite difference analysis) program to simulate the microstructure evolutions of two commercial plain carbon steels during hot strip rolling. Recently, based on a 2-D finite element method, Serajzadeh [7–9] presented a mathematical model to predict the thermal history and microstructure changes during hot rolling. Zhang and co-workers [10] carried out the 2-D finite element analysis of the thermal and metallurgical behavior of the strip during the hot finishing rolling process.

Since the application of 3-D models involves long computational time, most of previous works have concentrated on the 2-D analysis of microstructure evolution during hot rolling. Compared with 3-D models, 2-D models cannot exactly analyze

* Corresponding author. Tel.: +86 411 84706087; fax: +86 411 84709284.
*E-mail addresses:* chongxiang39@yahoo.com.cn (C.-x. Yue), commat@mail.dlut.edu.cn (L.-w. Zhang).

0307-904X/$ - see front matter © 2009 Elsevier Inc. All rights reserved.
doi:10.1016/j.apm.2009.12.001

the plastic deformation of rolled piece. Recently, with the rapid development of computer, the 3-D analysis of microstructure evolution has been applied widely to model hot upsetting, hot forging and hot forming process by many authors [11–18]. The applications are helpful to the 3-D analysis of hot rolling. In this paper, four 3-D finite element models are developed to simulate the distribution and evolution of different field-variables during the whole rod rolling process of GCr15 steel, such as effective strain, effective strain rate and temperature. Taking the simulated results and the microstructure evolution models of the steel into account, this paper designs a FORTRAN program to predict the evolution of recrystallization behavior and austenite grain size during the hot rod rolling of GCr15 steel.

## 2. FEM models

Fig. 1 shows the layout of rolling mills for the hot rod rolling of GCr15 steel in Dongbei Special Steel Group, China. The rolling process from the 1st pass to the 18th pass consists of three successive rolling stages, rough rolling, intermediate rolling and finishing rolling. All rollers are individually driven with an alternative vertical and horizontal arrangement. GCr15 steel is rolled from a 150 mm × 150 mm square billet to a rod with the diameter of 15 mm after passing 18 passes. The billet is rolled from square to box–square–oval–round during the first four passes, and then is deformed as oval-round at every two passes. Based on the commercial FE software MSC.Marc, the paper develops four 3-D finite element models to simulate the hot rod rolling. The first model is used to simulate the descaling stage and rough rolling stage as shown in Fig. 2. The front six passes and back four passes of intermediate rolling are simulated by the second model and the third one respectively. And the paper uses the fourth model to simulate the finishing rolling. In order to keep the continuity of simulated results, the data transmission from a model to the next model is completed by the data transfer technique [19,20]. In all models, rolled piece is defined as a deformation body and rollers are defined as rigid bodies. The roller dimensions and velocity are set according to practical condition. Owing to the symmetry, a quarter of rolled piece is included in every model. The quasi static analysis is adopted in the simulation. A pushing rigid body is introduced into the model. The rigid body whose speed is controlled by MSC.Marc subroutine is employed to push the rolled piece moving to next stand during the interpass period [19].

The material is a typical GCr15 steel. The chemical composition is 0.99%C, 0.24%Si, 0.31%Mn, 0.01%P, 0.003%S, 1.44%Cr, 0.05%Ni, 0.12%Cu, 0.02%Mo and the balance Fe. The material flow behavior is determined by the flow stress data gained in thermo-mechanical simulation experiments of the steel [21,22]. It is assumed that the material is isotropic and the yielding behavior follows the Von Mises yield criterion. And mechanical properties and thermal expansion coefficient of the material are provided by Dongbei Special Steel Group. The initial temperature is 1045 °C. The heat flow on the rolled piece is given by the numerical solution of the non-steady heat conduction equation:

$$\frac{\partial}{\partial x}\left(\lambda\frac{\partial T}{\partial x}\right)+\frac{\partial}{\partial y}\left(\lambda\frac{\partial T}{\partial y}\right)+\frac{\partial}{\partial z}\left(\lambda\frac{\partial T}{\partial z}\right)+\dot{q}=\rho C_p\frac{\partial T}{\partial t}, \tag{1}$$

where $C_p$ and $\lambda$ are temperature dependent functions, $C_p$ is the specific heat, $\lambda$ is the thermal conductivity, $\rho$ is the density, and $\dot{q}$ is the internal heat intensity.

$$\dot{q}=k\bar{\sigma}\cdot\dot{\bar{\varepsilon}}, \tag{2}$$

where $k$ is the conversion efficiency of mechanical work to heat, which is assumed to be 0.90.

The heat transfer mechanism during hot rolling process is complex. Heat generation occurs owing to the energy of friction work at the contact surface. The cooling conditions that exist in the practical rolling process, such as water descaling before the first stand, water cooling between stands, cooling in air, and heat exchanges between rolled piece and rollers, must be considered too. So the following boundary conditions are used to solve Eq. (1).

(a) On the symmetric planes, it is supposed that the heat flux is zero.

$$\frac{\partial T}{\partial r}=0. \tag{3}$$

(b) On the free surface of rolled piece, the thermal conditions agree with the equation.

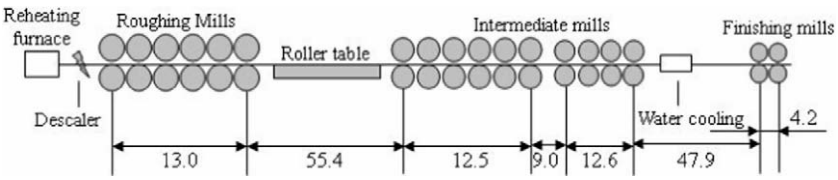


**Fig. 1.** Layout of rolling mills (dimension unit: m).

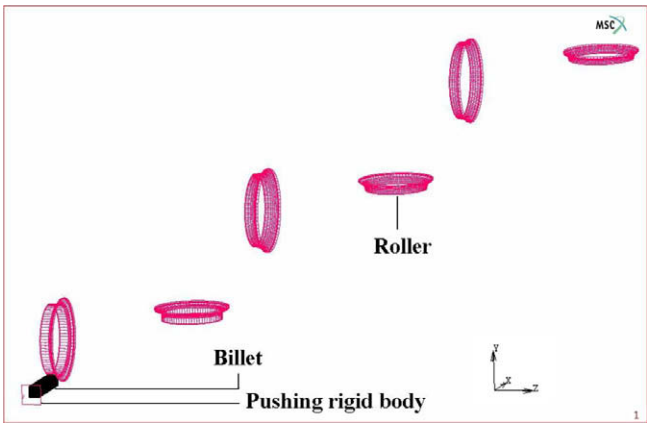


**Fig. 2.** The first finite element model for the descaling stage and rough rolling stage.

$$-\lambda\frac{\partial T}{\partial r} = h(T_s - T_m), \tag{4}$$

where $h$ is a total heat transfer coefficient (70 W m$^{-2}$ K$^{-1}$) which comprises a heat transfer coefficient by convection and a radiant heat transfer coefficient when rolled piece is between stands. $h$ represents an effective heat transfer coefficient during water descaling and water cooling process (4–8 kW m$^{-2}$ K$^{-1}$). And $h$ is the contact heat exchange coefficient (9.5 kW m$^{-2}$ K$^{-1}$) when rolled piece contacts with rollers. $T_s$ is the surface temperature of rolled piece. $T_m$ is the temperature of contact medium.

The shear friction model is used to model the friction phenomenon during the rolling process. The friction heat $q$ between rolled piece and rollers is written as follows:

$$q = k_f|\tau \cdot \Delta v|, \tag{5}$$

where $\tau$ is the friction force, $\Delta v$ is relative velocity of movement, and $k_f$ is the distribution coefficient of heat. As for the hot rolling, $k_f$ is equal to 0.5. The value means that the total friction heat is fairly assigned to the contact surfaces of both rolled piece and rollers.

## 3. Microstructure evolution models

Austenite grain evolution during hot rolling is one of the physical metallurgical phenomena, and its evolution pattern mainly consists of four types, namely, dynamic recrystallization (DRX) during hot deformation, metadynamic recrystallization (MDRX) and static recrystallization (SRX) after deformation, as well as grain growth after complete recrystallization when the dynamic and static recoveries are ignored [23,24]. When steel in the austenite phase is deformed at high temperature, the flow stress rises to a maximum and then falls to a steady state. The softening is called "dynamic recrystallization". DRX involves the nucleation and growth of new grains when the strain during deformation exceeds a critical value. The deformed grains will be represented by new equiaxed grains when DRX is complete. If the strain is less than the steady state strain, DRX is not complete. After the deformation, recrystallization continues until new equiaxed grains represent all deformed grains finally. The recrystallization is MDRX. The same as DRX, SRX is a nucleation and growth process of new strain-free grains too, but the process starts and completes after deformation. When the recrystallization is complete, the new structure is meta-stable and grain growth will take place to reduce grain boundary area per unit volume [18]. In order to investigate the recrystallization and grain growth behavior of GCr15 steel during hot rolling, the hot compression and annealing tests are preformed on the Gleeble-3800 thermo-mechanical simulation machine [25,26]. According to experimental results, a set of mathematical models which can predict the recrystallization and grain growth behavior of GCr15 steel during hot rolling are obtained [25].

The DRX behavior of GCr15 steel can be modelled by the following equations [2,22,25–28].

$$\varepsilon_c = 3.55 \times 10^{-3} d_0^{0.22} \dot{\varepsilon}^{0.19} \exp\left(\frac{4461.0}{T}\right), \tag{6}$$

$$X_d = 1 - \exp\left[-0.693\left(\frac{t_d}{t_{0.5/d}}\right)^2\right], \tag{7}$$

$$t_{0.5/d} = 3.49 \times 10^{-2} \dot{\varepsilon}^{-0.95} \exp(2486.0/T), \tag{8}$$

$$d_d = 3.4 \times 10^4 \dot{\varepsilon}^{f(T)} \exp(g(T)), \tag{9}$$

where

$$f(T) = -1.09505 + 0.08602 \times 10^{-4}T + 1283.3/T, \tag{10}$$

$$g(T) = -1.82459 \times 10^{-5}T - 9189.0/T, \tag{11}$$

where $\varepsilon_c$ is the critical strain for the onset of DRX, $d_0$ is the initial grain size, $\dot{\varepsilon}$ is strain rate, $T$ is the absolute temperature, $X_d$ is dynamic recrystallized fraction, $t_d$ is deformation time after the critical strain, $t_{0.5/d}$ equals to $t_d$ for 50% recrystallization, $d_d$ is grain size after complete DRX.

Typically, the evolution of MDRX is discussed in terms of recrystallization kinetics and meta-dynamic recrystallized grain size as follows [13,17,29–31]:

$$X_m = 1 - \exp\left[-0.693\left(\frac{t_m}{t_{0.5/m}}\right)^2\right], \tag{12}$$

$$t_{0.5/m} = 0.042\varepsilon^{-0.045}\dot{\varepsilon}^{-0.644}d_0^{0.207}\exp(3088.9/T), \tag{13}$$

$$d_m = 393.3\varepsilon^{-0.76}\dot{\varepsilon}^{-0.016}d_0^{0.129}\exp(-4757.4/T), \tag{14}$$

where $X_m$ is meta-dynamic recrystallized fraction, $t_m$ is the delay time after deformation, $t_{0.5/m}$ equals to $t_m$ for 50% recrystallization, $d_m$ is grain size after complete MDRX.

In this paper, the following equations have been used to describe the evolution of SRX [6,32–37].

$$X_s = 1 - \exp\left[-0.693\left(\frac{t_s}{t_{0.5/s}}\right)^2\right], \tag{15}$$

$$t_{0.5/s} = 5.396 \times 10^{-10}\varepsilon^{-1.5}\dot{\varepsilon}^{-0.373}d_0^{1.47}\exp(16203.6/T), \tag{16}$$

$$d_s = 430.7\varepsilon^{-0.428}\dot{\varepsilon}^{-0.093}d_0^{0.146}\exp(-4461.5/T), \tag{17}$$

where $X_s$ is static recrystallized fraction, $t_s$ is the delay time after deformation, $t_{0.5/s}$ equals to $t_s$ for 50% recrystallization, $d_s$ is grain size after complete SRX.

The equation for grain growth is described by the following equation [38–41]:

$$d_t^{2.77} - d_0^{2.77} = 3.12 \times 10^{19}\exp(-4.58 \times 10^5/RT)t, \tag{18}$$

where $d_t$ is the average grain size at time $t$, and $R$ is the general gas constant.

By coupling above equations for the recrystallization and grain growth behavior, a FORTRAN program is designed to predict the evolution of recrystallization behavior and austenite grain size during the rolling process of the steel. For the first pass rolling, an initial austenite grain size is assigned to the program. Because the effect of different initial grain sizes will disappear after several sufficient cycles of recrystallization during multi-pass continuous rolling [4,42–44], modelling microstructure evolution during the multi-pass rolling of GCr15 rod does not require an accurate measure of initial grain size. In the program, the initial austenite grain size before the first pass rolling is assumed to be 200 μm.

The flowchart of the program is shown in Fig. 3. It is divided into two parts: rolling and interpass. In rolling period, the grain size equals to the initial grain size when strain is smaller than the critical strain. If strain is greater than the critical strain, DRX takes place. The program calculates $X_d$ and $d_d$ step by step. Then the average grain size, $d$, is calculated according to Eq. (19). This computational process continues till the deformation period is over. In interpass time, if recrystallized fraction is more than 95%, the recrystallization is assumed to be complete and grain growth is calculated according to Eq. (18). Otherwise MDRX or SRX will occur. The program calculates $X_m$, $d_m$, $X_s$ and $d_s$ step by step. Then the average grain size, $d$, is calculated according to Eq. (20) or Eq. (21). This process continues till the interpass time is over. Predicted average grain size is regarded as the initial grain size during next pass rolling, and retained strain, $\varepsilon_r$, is calculated.

$$\text{DRX}: \quad d = d_dX_d + (1 - X_d)d_0, \tag{19}$$

$$\text{MDRX}: \quad d = d_dX_d + (1 - X_d)X_md_m + (1 - X_d)(1 - X_m)d_0, \tag{20}$$

$$\text{SRX}: \quad d = d_sX_s + (1 - X_s)d_0. \tag{21}$$

## 4. Industrial trials

The verification and calibration of simulated results have been performed by comparing calculated values with actual data measured during the hot rolling of GCr15 rod in Dongbei Special Steel Group, China. Measurement of on-line rod surface temperatures were carried out at different places of stands 1–10 with a pyrometer during the actual rolling process. Specimens for austenite microstructure analysis were cut using the crop shears at various stages of the rolling process, and water quenched immediately to retain the crystal boundary of high temperature austenite microstructure. After etched with an aqueous solution of picric acid at 50–60 °C, the microstructures at different parts of the rolled piece were examined by optical microscopy. Fig. 4 shows the microstructures at the surface (near Node b in Fig. 12) of rolled piece before 7th pass and

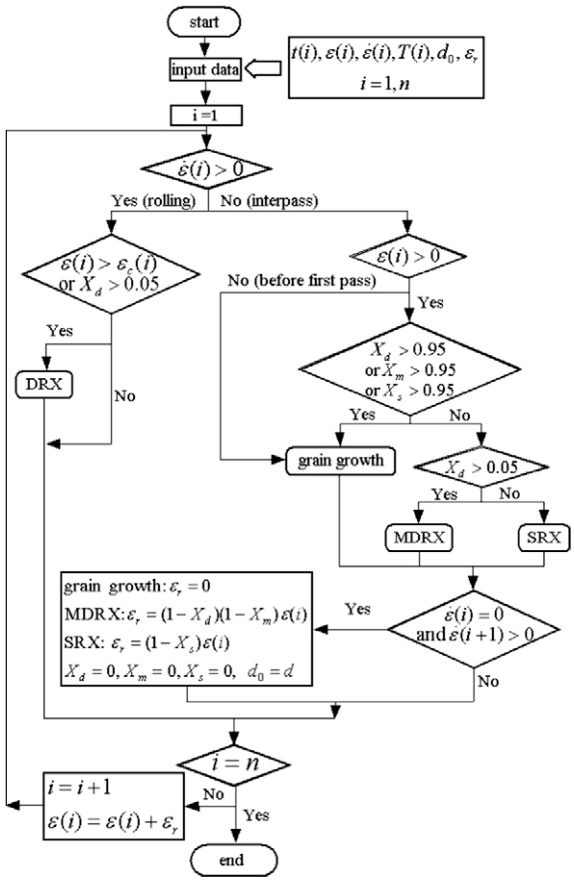


**Fig. 3.** Flowchart of the FORTRAN program.

after 18th pass. It can be seen that the crystal boundary of austenite microstructure is very clear. Then the grain sizes were measured by the linear intercept method. The average values of the grain sizes at the center and surface of rolled piece are 36.4 μm and 15.7 μm before 7th pass, 24.3 μm and 20.4 μm before 13th pass, 18.3 μm and 18.7 μm after 18th pass, respectively. Due to lack of number of the crop shears installed in the rod mill, experimental microstructure was only obtained at limited location. The measured values of grain sizes can be used to validate the simulated results of the evolution of austenite grain size during the hot rod rolling of GCr15 steel.

## 5. Results and discussions

It is difficult to analyze quantitatively the whole rolling process by the traditional methods because of its complicated deformation mechanism. In the present study, the transient evolution of various variables has been acquired with the aid of the finite element models and the FORTRAN program designed by the authors.

### 5.1. Field-variables distribution

Temperature is one of the most important variables governing the behavior of metals under hot-working conditions [5]. During hot rolling, the temperature of rolled piece depends on various factors such as initial temperature, the amount of plastic deformation, the coefficients of heat transfer among rolled piece and other objects, etc. [45]. Figs. 5 and 6 show the temperature distributions in the rolled piece at the third and 17th pass. It can be seen that surface temperature drops rapidly after the third pass rolling. Meanwhile, the surface temperature increases in the 17th roll gaps. The reasons for the change of temperature will be explained in detail in Section 5.2.

DRX occurs during hot rolling when the critical strain is reached. So strain has a direct effect on the recrystallization behavior in the rolled piece. Fig. 7 illustrates the field plot of total effective strain in the rolled piece at the third pass. It can be easily found that the deformation of the rolled piece is inhomogeneous, and total strain becomes larger after rolling. By subtracting the strain before the pass rolling from total effective strain, the evolution of effective strain during every pass can be obtained. Apart from temperature and strain, strain rate is also an important factor that influences the deformation

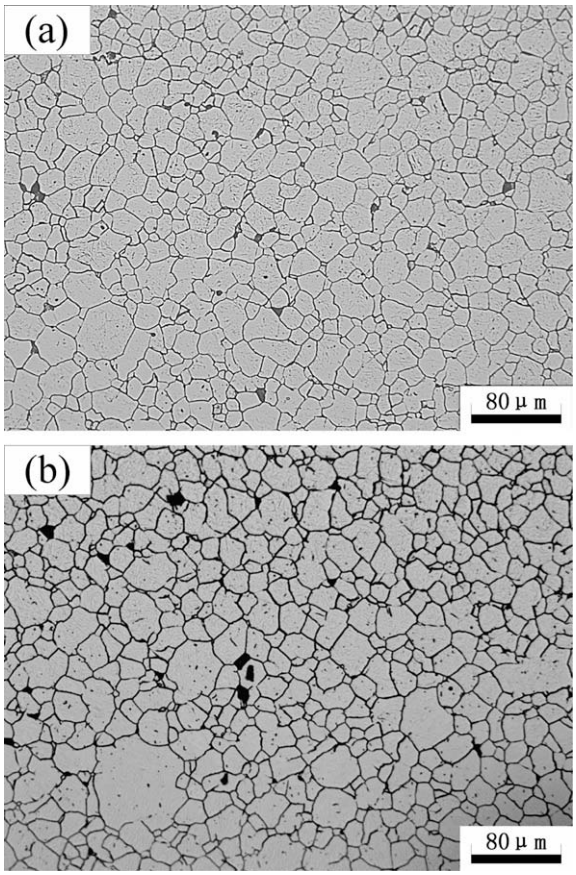


**Fig. 4.** Austenite microstructures at the surface of rolled piece (a) before 7th pass and (b) after18th pass.

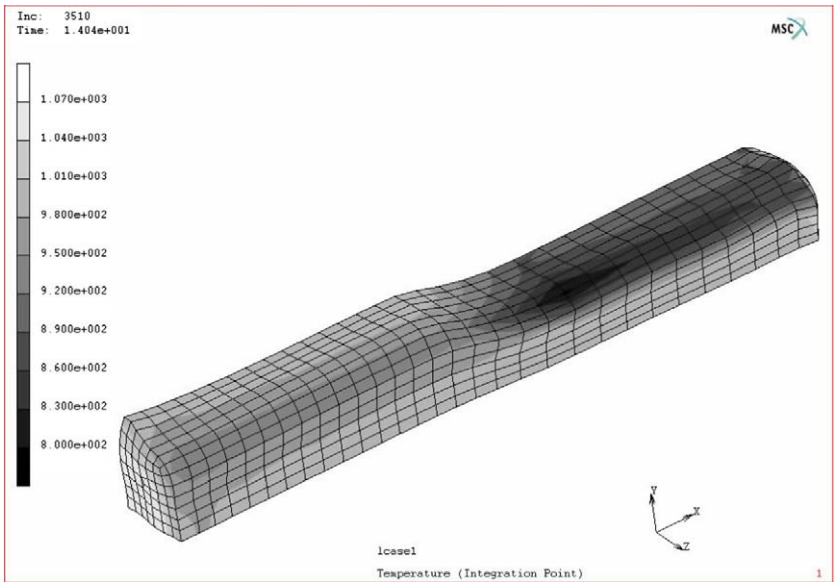


**Fig. 5.** Temperature distribution in the rolled piece at the third pass.

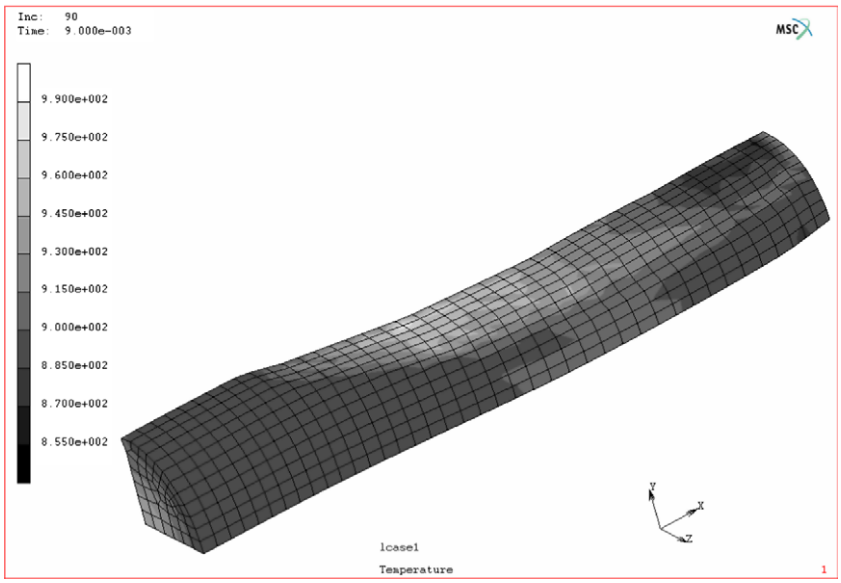


**Fig. 6.** Temperature distribution in the rolled piece at the 17th pass.

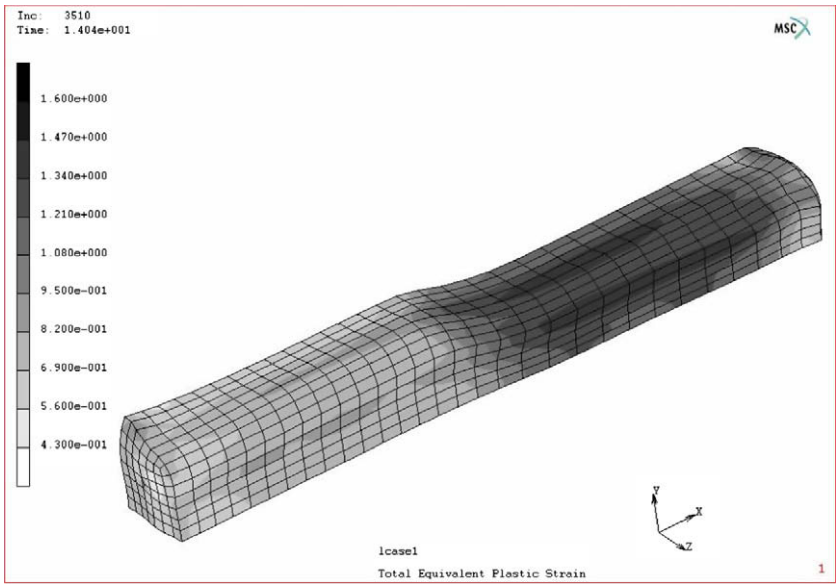


**Fig. 7.** Distribution of total effective strain in the rolled piece at the third pass.

and microstructure evolution of material [45]. The field plot of effective strain rate in the rolled piece at the third pass is presented in Fig. 8. Obviously, the effective strain rate changes dramatically around the rolling deformation region and the value of the rate is zero at other parts of the rolled piece.

### 5.2. Temperature evolution

Temperature evolution predicted by the present finite element models is illustrated in Fig. 9. The change of surface temperature is complex. Before the first pass, the surface temperature decreases because of heat convection to descaling water. During 1–12 passes, the surface temperature drops rapidly in the roll gaps due to the relatively cold roller and rises slowly thereafter. During 13–18 passes, the mill speed is very fast and the heat conduction to the cold roller becomes very small. So the surface temperature increases rapidly in the roll gaps because of deformation heat, and then decreases slowly because of the radiation to air. Especially, the surface temperature drops obviously between the 16th and 17th pass because of the

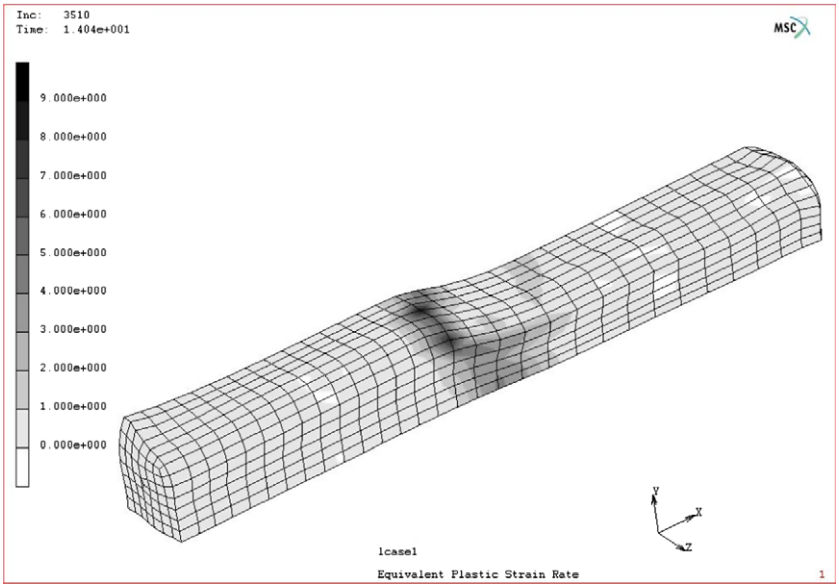


**Fig. 8.** Distribution of effective strain rate in the rolled piece at the third pass.

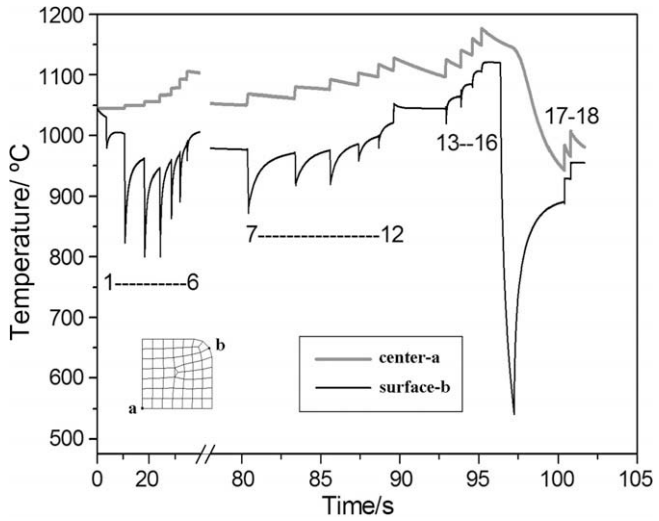


**Fig. 9.** Temperature evolution predicted by the present finite element models.

convection to cooling water, as shown in Fig. 1. The center temperature of rolled piece increases in the roll gaps due to the deformation heat, and then decreases slowly in interpass time due to the heat loss by convection and radiation.

To verify the simulated results, temperature measurements were conducted on the area near the profile midline of the billet. For the temperature measured at each stand from the head to the tail of a billet, measured values are shown as a range. The comparison between measured and calculated temperatures is shown in Fig. 10. It is clear that surface temperatures of billet calculated by FEM agree well with the measurement.

### 5.3. Microstructure evolution

Fig. 11 presents the recrystallized fraction of austenite at the center of rolled piece during the hot rolling of GCr15 rod. It can be seen that SRX occurs during the first pass, and then DRX and MDRX take place during other passes. The evolution of simulated austenite grain size during the whole rolling process is presented in Fig. 12. It can be seen that the grains are refined greatly and the deviation of grain sizes between center and surface reaches the maximum gradually during the first three passes. Subsequently, the grain sizes do not change largely, but the deviation of grain sizes decreases gradually by the actions of deformation refinement and interval grain growth during the later passes. After the 17th pass, the austenite

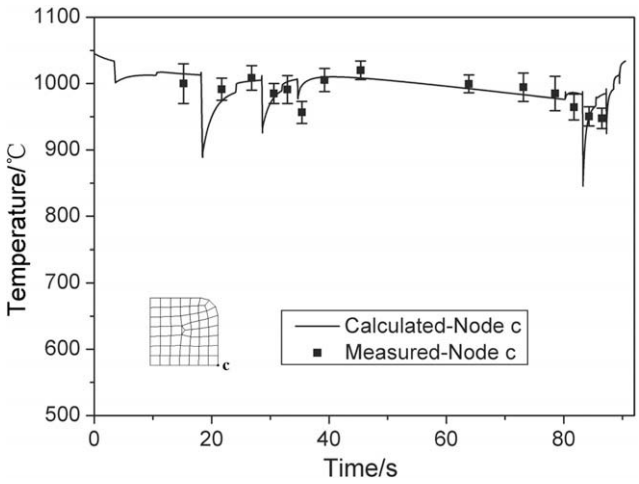


**Fig. 10.** Comparison of measured surface temperatures with calculated results.

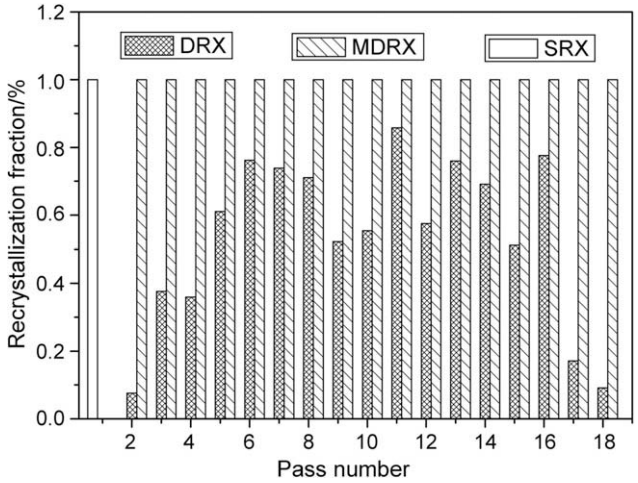


**Fig. 11.** Predicted recrystallized fraction in the center of rolled piece during hot rolling.

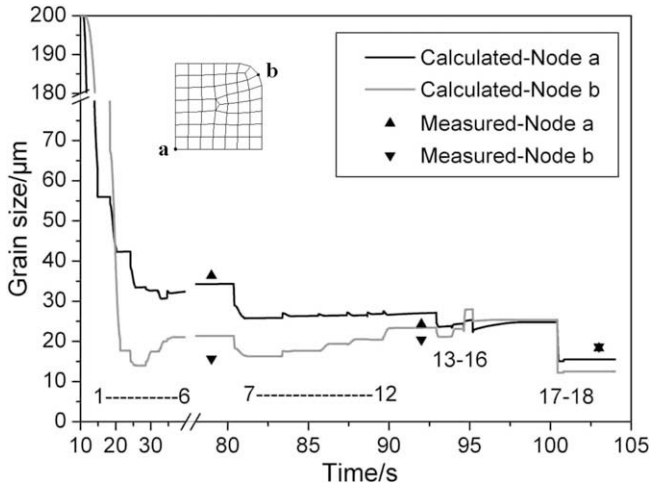


**Fig. 12.** Comparison of measured grain sizes with calculated results.

grains are refined obviously again. This phenomenon, in fact, can be attributed to the reduced statically recrystallized grain size when rolling temperature becomes lower before the 17th pass because of the convection to cooling water, as described in Fig. 9. In order to investigate the tendency of microstructure evolution during the hot rolling of GCr15 rod and verify the designed program in this paper, the austenite grain sizes of experiment and simulation are compared, as shown in Fig. 12. It is observed that simulated results are close to experimental results. Microstructure evolution during multi-pass hot rolling is more complicated than the evolution during hot compression tests, so the microstructure evolution models obtained on the basis of the results of compression tests are not able to exactly reflect real evolution of microstructure during GCr15 rod rolling. Take the factor into account, the difference between simulation and experiment is reasonable. In addition, the trend of simulation is in good agreement with experiment.

## 6. Conclusions

Four 3-D finite element models for forecasting the distribution and evolution of different field-variables during the hot rolling of GCr15 rod have been developed. The paper simulates the whole rolling process of GCr15 rod by these models. Based on the simulated results and the microstructure evolution models of the steel, a FORTRAN program has been programmed to calculate the evolution of recrystallization behavior and austenite grain size during the whole rolling process of GCr15 rod. Simulated results of surface temperature are in good agreement with those of experiment, and calculated grain sizes are close to measured data.

## Acknowledgements

The authors appreciate the financial support received from Dalian City Government (Liaoning Province, China) and Dongbei Special Steel Group Corporation.

## References

[1] C.M. Sellars, Mater. Sci. Technol. 6 (1990) 1072.
[2] W.P. Sun, E.B. Hawbolt, ISIJ Int. 37 (1997) 1000.
[3] G.B. Tang, Z.D. Liu, H. Dong, J. Iron. Steel. Res. Int. 14 (4) (2007) 49.
[4] C.M. Sellars, J.A. Whiteman, Met. Sci. 13 (1979) 187.
[5] C.M. Sellars, Meter. Sci. Technol. 1 (1985) 325.
[6] R. Kuziak, M. Glowacki, M. Pietrzyk, J. Mater. Process. Technol. 60 (1996) 589.
[7] S. Serajzadeh, H. Mirbagheri, A.K. Taheri, J. Mater. Process. Technol. 125/126 (2002) 89.
[8] S. Serajzadeh, Int. J. Mach. Tool. Manu. 43 (2003) 1487.
[9] S. Serajzadeh, Mater. Sci. Eng. A 448 (2007) 146.
[10] Z.D. Qu, S.H. Zhang, D.Z. Li, Acta Metall. Sin. (Engl. Lett.) 20 (2) (2007) 79.
[11] Y.C. Lin, M.S. Chen, J. Zhong, Mater. Des. 30 (2009) 908.
[12] Y.C. Lin, M.S. Chen, J. Zhong, Comput. Mater. Sci. 43 (2008) 1117.
[13] J.T. Yeom, C.S. Lee, J.H. Kim, Mater. Sci. Eng. A 449/451 (2007) 722.
[14] F.S. Du, M.T. Wang, X.T. Li, J. Mater. Process. Technol. 187/188 (2007) 591.
[15] W.G. Jiang, G.C. Wang, S.Q. Lu, J. Mater. Process. Technol. 182 (2007) 274.
[16] J.R. Cho, H.S. Jeong, D.J. Cha, J. Mater. Process. Technol. 160 (2005) 1.
[17] Y.S. Na, J.T. Yeom, N.K. Park, J. Mater. Process. Technol. 141 (2003) 337.
[18] Y.S. Jang, D.C. Ko, B.M. Kim, J. Mater. Process. Technol. 101 (2000) 85.
[19] S.Y. Yuan, L.W. Zhang, S.L. Liao, J. Mater. Process. Technol. 209 (2009) 2760.
[20] S.L. Liao, L.W. Zhang, S.Y. Yuan, J. Univ. Sci. Technol. B 15 (2008) 412.
[21] C.X. Yue, S.L. Liao, L.W. Zhang, Mater. Sci. Eng. A 499 (2009) 177.
[22] S.L. Liao, L.W. Zhang, C.X. Yue, J. Cent. South Univ. Technol. 15 (2008) 575.
[23] X.T. Li, M.T. Wang, F.S. Du, J. Iron. Steel. Res. Int. 15 (4) (2008) 42.
[24] X.T. Li, M.T. Wang, F.S. Du, Mater. Sci. Eng. A408 (2005) 33.
[25] C.X. Yue, S.L. Liao, L.W. Zhang, Comput. Mater. Sci. 45 (2009) 462.
[26] C.X. Yue, S.L. Liao, L.W. Zhang, Mater. Res. Innov. 12 (4) (2008) 213.
[27] J.J. Park, J. Mater. Process. Technol. 113 (2001) 581.
[28] A. Yanagida, J. Yanagimoto, Mater. Sci. Eng. A 487 (2008) 510.
[29] A. Dehghan-Manshadi, M.R. Barnett, P.D. Hodgson, Mater. Sci. Eng. A 485 (2008) 664.
[30] G. Shen, S.L. Semiatin, R. Shivpuri, Metall. Mater. Trans. A 26A (1995) 1795.
[31] Z.H. Zhang, Y.N. Liu, X.K. Liang, et al, Mater. Sci. Eng. A 474 (2008) 254.
[32] M. Glowacki, R. Kuziak, Z. Malinowski, J. Mater. Process. Technol. 53 (1995) 159.
[33] E. Anelli, ISIJ Int. 32 (1992) 440.
[34] H. Grass, C. Krempaszky, T. Reip, Comput. Mater. Sci. 28 (2003) 469.
[35] A. Kumar, S. Jha, V. Ramaswamy, Steel Res. 64 (1993) 210.
[36] H. Grass, C. Krempaszky, T. Reip, Comput. Mater. Sci. 28 (2003) 469.
[37] Z. Gronastajski, J. Mater. Process. Technol. 157–158 (2004) 165.
[38] K. Farrell, P.R. Munroe, Scr. Mater. 35 (1996) 615.
[39] W.M. Tang, Z.X. Zheng, H.J. Tang, Intermetallics 15 (2007) 1020.
[40] W. Li, K. Xia, Mater. Sci. Eng. A 329/331 (2002) 430.
[41] R. Ren, Y.C. WU, W.M. Tang, Trans. Nonferr. Met. Soc. China 18 (2008) 66.
[42] S.R. Wang, A.A. Tseng, Mater. Des. 16 (6) (1995) 315.
[43] T. Siwechi, ISIJ Int. 32 (1992) 368.
[44] J.H. Beynon, C.M. Sellars, ISIJ Int. 32 (1992) 359.
[45] M.T. Wang, X.T. Li, F.S. Du, Mater. Sci. Eng. A 391 (2005) 305.